

Auralizing position-dependent abatements for a moving, extended source using a reference-case recording

Project: Good sound environment in station communities
(God ljudmiljö i stationssamhällen)

Jens Forssén, August 2019

Report
Division of Applied Acoustics
Department of Architecture and Civil Engineering
Chalmers University of Technology



CHALMERS UNIVERSITY OF TECHNOLOGY
Applied Acoustics
412 96 Göteborg, Sweden
Visiting address: Sven Hultins gata 8 A
Telephone: +46-31-772 8604 Fax: +46-31-772 22 12
Reg. No: 556479-5598
E-mail: jens.forssen@ta.chalmers.se

INTRODUCTION

Based on a recording (mono, binaural, sound field, or other format) from a train pass-by (or incoming/leaving train) in a reference situation (e.g., open terrain), we would like to emulate the effect of a noise abatement (e.g., a low-height screen, wheel damper, rail damper, etc.).

Since using a single point source to model a train (consisting of a set of railroad vehicles) is usually insufficient (except for very distant receivers), contrary to e.g. a light road vehicle, it is of interest to use an extended source or multiple sources at the same time as keeping the model simple. In addition, the abatement may involve an angular dependent noise reduction (i.e., for a fixed receiver position, dependent on source position on the train).

METHOD

A set of sources, s_i , $i = 1 \dots N$, is placed along the length of the train (and possibly longer, e.g. to model extended rail radiation). The received sound pressure, p , as function of time, t , at a spatial point j may then be written as a sum over the individual sources' contributions:

$$p_j(t) = \sum_{i=1}^N \int_0^\infty s_i(t - \tau) d_{ij}(t - \tau) h_{ij}(\tau) d\tau. \quad (1)$$

Here, d_{ij} is a directivity function and h_{ij} is the impulse response function from source i to receiver j . (Note that the directivity function may be used for approximating source directivity and convection effect, i.e. the amplitude change due to a moving source's direction and Mach number, as well as the receiver's directional sensitivity, e.g. for binaural signals.)

Assuming that the sources are temporarily stationary in space (further discussed below), a frequency domain equivalent of Eq. (1) may be written as

$$P_j(f) = \sum_{i=1}^N S_i(f) D_{ij}(f) H_{ij}(f)$$

where f is the frequency of the sound.

By further assuming uncorrelated sources, we can write:

$$|P_j(f)|^2 = \sum_{i=1}^N |S_i(f)|^2 |D_{ij}(f)|^2 |H_{ij}(f)|^2. \quad (2)$$

When the train moves with speed U along the x -axis during a time block Δt_b , each point source has moved a distance $\Delta x_b = U\Delta t_b$ along the x -axis. Using Eq. (2) to find $|P_j(f)|^2$ also for the updated train position, by assuming stationary source signals (i.e. $|S_i(f)|^2$ unchanged) but updated values of $|D_{ij}(f)|^2$ and $|H_{ij}(f)|^2$, inherently means neglecting effects of source movement, like the Doppler effect. Since the application of interest here concerns only a relative change between a reference and a new case, i.e. a ratio like $|P_j^{REF}(f)|/|P_j^{NEW}(f)|$, the spectral amplitude influence of the Doppler effect is diminished. (Note also that the Doppler effect of the reference recording will still be there, with the most audible contributions coming from the region of the train closest to the receiver.)

Instead of moving the sources in space we can move the receiver, which simplifies the notation. For each time block, the location of P_j , positioned at x_j is exchanged by P_{j+1} , positioned at x_{j+1} , where $x_{j+1} = x_j - U\Delta t_b$. Interpreting j as time steps ($j = 0, 1, 2, \dots$), we may write $x_j = x_0 - jU\Delta t_b$, where $j = 0$ at the starting position $x_0 = x_r$.

For each time step j , we can now define an insertion loss spectrum as

$$IL_j(f) = 20 \log \left(\frac{|P_j^{REF}(f)|}{|P_j^{NEW}(f)|} \right) \quad (3a)$$

i.e., from using Eq. (2),

$$IL_j(f) = 10 \log \left(\frac{\sum_{i=1}^N |S_i(f)|^2 |D_{ij}(f)|^2 |H_{ij}^{REF}(f)|^2}{\sum_{i=1}^N |S_i(f)|^2 |D_{ij}(f)|^2 |H_{ij}^{NEW}(f)|^2} \right). \quad (3b)$$

Using Eq. (3a) for a known insertion loss spectrum, the new sound pressure level spectrum can be given from the reference using:

$$20 \log(|P_j^{NEW}(f)|) = 20 \log(|P_j^{REF}(f)|) - IL_j(f)$$

Equation (3b) may be rewritten using a *point-to-point* insertion loss, which could originate from a measurement or a calculation, $IL_{ij}(f) = 20 \log(|H_{ij}^{REF}(f)|/|H_{ij}^{NEW}(f)|)$, resulting in

$$IL_j(f) = 10 \log \left(\frac{\sum_{i=1}^N |S_i(f)|^2 |D_{ij}(f)|^2 |H_{ij}^{REF}(f)|^2}{\sum_{i=1}^N |S_i(f)|^2 |D_{ij}(f)|^2 |H_{ij}^{REF}(f)|^2 10^{-IL_{ij}(f)/10}} \right). \quad (4)$$

TEST RESULTS

Assume for simplicity that the source strength is constant along the train ($S_i(f) = S(f)$ for all $i = 1 \dots N$) and that they are all omnidirectional ($D_{ij}(f) = 1$). (Improvements from these assumptions can be made using existing source models in literature, or more advanced models.) Applying these assumptions in Eq. (4), we get

$$IL_j(f) = 10 \log \left(\frac{\sum_{i=1}^N |H_{ij}^{REF}(f)|^2}{\sum_{i=1}^N |H_{ij}^{REF}(f)|^2 10^{-IL_{ij}(f)/10}} \right). \quad (5)$$

Or, in terms of a factor, F_j , to multiply on the amplitude:

$$F_j(f) = \sqrt{\frac{\sum_{i=1}^N |H_{ij}^{NEW}(f)|^2}{\sum_{i=1}^N |H_{ij}^{REF}(f)|^2}} = \sqrt{\frac{\sum_{i=1}^N |H_{ij}^{REF}(f)|^2 10^{-IL_{ij}(f)/10}}{\sum_{i=1}^N |H_{ij}^{REF}(f)|^2}}. \quad (6)$$

If preferable, the above may also be formulated using a point-to-point amplification, $G_{ij} = 10^{-IL_{ij}(f)/20}$, as:

$$F_j(f) = \sqrt{\frac{\sum_{i=1}^N |H_{ij}^{REF}(f)|^2 G_{ij}^2(f)}{\sum_{i=1}^N |H_{ij}^{REF}(f)|^2}}. \quad (7)$$

For cases with different source types, e.g. located at different heights, Eq. (7) can be rewritten for clarity. For an example with three sources (denoted with numerals 1, 2 and 3), we could write as follows.

$$F_j(f) = \sqrt{\frac{\sum_{i=1}^N w_1(f) |H_{1,ij}^{REF}(f)|^2 G_{1,ij}^2(f) + w_2(f) |H_{2,ij}^{REF}(f)|^2 G_{2,ij}^2(f) + w_3(f) |H_{3,ij}^{REF}(f)|^2 G_{3,ij}^2(f)}{\sum_{i=1}^N w_1(f) |H_{1,ij}^{REF}(f)|^2 + w_2(f) |H_{2,ij}^{REF}(f)|^2 + w_3(f) |H_{3,ij}^{REF}(f)|^2}}. \quad (8)$$

Here, w_1, w_2, w_3 , are used to weigh the contributions in power of the three sources. (See also Figure 2.)

In what follows, Eq. (8) is applied for a simplified model case with a thin, hard, low-height screen omitting the reflections in the ground surface. The screen, with its top at height 0.7 m above the ground plane, is placed at a range of 0.9 m from the source(s). The receiver is located at the range 6.7 m from the source(s), at height 1.2 m above the ground plane.

The three sources used are the following.

1. Low source (0.01 m above ground plane) is "rail noise"
2. Mid source (0.50 m above ground plane) is "wheel noise", including bogie noise
3. High source (3-5 m above ground plane) represents a collection of other sources (fans, aerodynamic sources from pantograph, etc.); this source is assumed to be unshielded, i.e. corresponding part of the original signal is left unfiltered.

An example of the relative contributions of the respective sources is shown in Figure 2, normalized such that the sum equals 1 for each frequency. For the final tool, the used input data are from measurements of X2000 trains: for the high source given by Ref. [1] (Table 3.6, covering driving speeds of 30–320 km/h) and, for the other sources, by Ref. [2] (Tables 4.3–4.4, covering driving speeds of 150–300 km/h). For driving speeds lower than the covered range, the power at the lowest tabulated driving speed is used. For adapting the source modelling to other train types, other sets of data could easily be inserted when available. Furthermore, it should be noted that the modelling made here assumes monopoles whereas the real sources have partly a dipole character, which could be refined in future implementations.

The sources, being at different heights, are also linked with different insertion losses. The insertion loss data are given as function of frequency as well as of translation in space along the rail track compared with the receiver (Δy). Concerning discretization, a step size of $\Delta y = 1$ m is used here. In Figure 3 an example is shown for the insertion loss. It can be noted that the insertion loss increases with frequency but decreases with Δy .

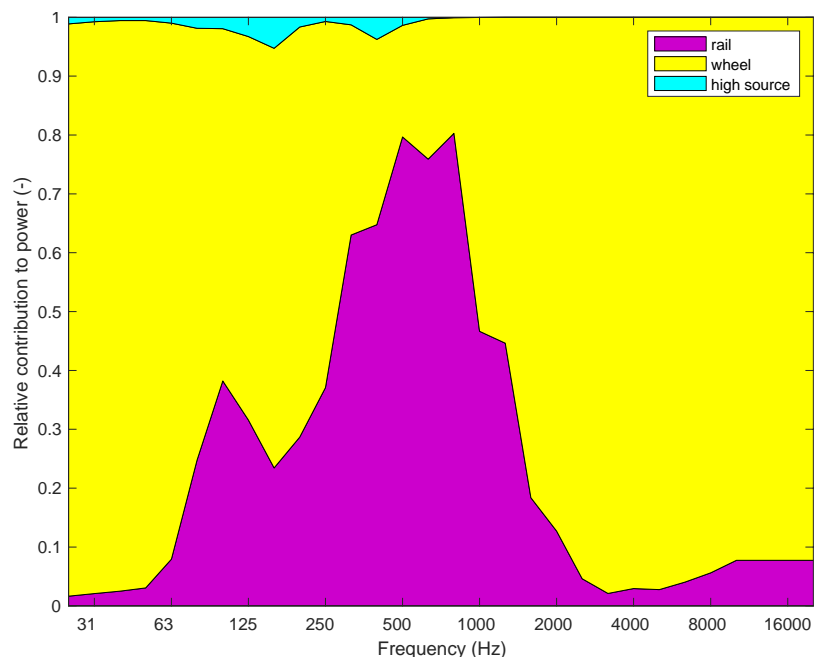


Figure 2. Example of relative power contribution for three sources.

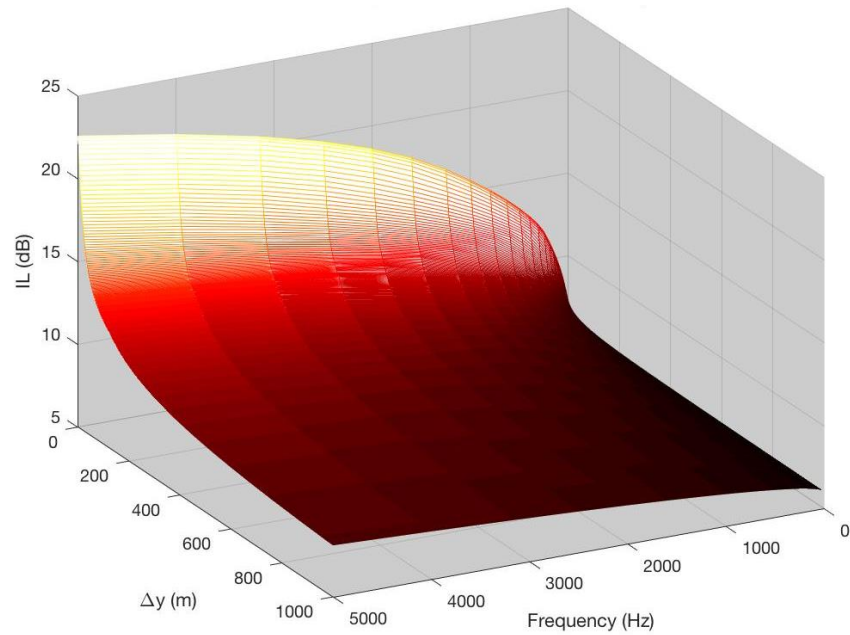


Figure 3. Plotted example of insertion loss (IL) data as function of frequency and translated distance along the rail track (Δy).

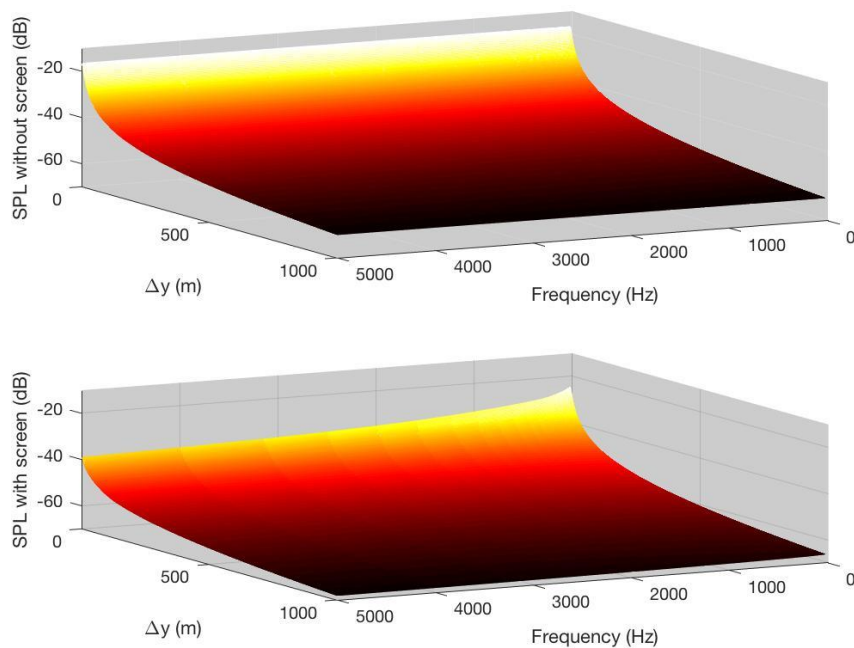


Figure 4. Sound pressure levels without and with screen (top respective bottom panel), corresponding to the insertion loss plotted in Figure 3, as function of frequency and translated distance along the rail track (Δy).

In the auralization methodology, the above modelling is applied to recorded binaural signals. When the insertion loss data or the source power contribution data are not available at sufficiently high frequencies for the sound synthesis (31.5 kHz used here), their respective values are taken as that available at the highest frequency. This generally causes an underestimation of the abated noise levels since the barrier insertion losses tend to increase with frequency. However, the numerical modelling is made up to 5 kHz, whereby the

dominating spectral part of the noise is preserved and the error can be argued to be of small influence.

As a test case, the above modelling is applied to a recorded binaural signal (using a dummy head with a microphone at the opening of each ear) for a Regina train passing at a constant speed of 75 km/h (21 m/s). Listening at the original recording and the processed one, the noise barrier effect can be heard clearly and the processed signal during passage sounds realistic.

Another test case is investigated where the low-height screen of the previous example is given a finite length. At a distance of 5 m further down the rail from the receiver, the screen ends. (Note that the diffraction due to the vertical edge of the screen is not modelled, which is a simplifying assumption made here, but could be included if wanted.) The level sounds right, but the next step would involve altering the binaural balance, via the directivity, effectively to reduce the right-ear signal more than the left-ear signal after the train head has passed the end of the screen.

In order to alter the binaural balance, e.g. for the case of a finite-length screen, as mentioned above, binaural weights are introduced as function of frequency and angle. The angular variation is interpolated into translated distance along the rail track (Δy). Denoting the energy-proportional binaural weights as $B_{ij}(f)$, the updated version of Eq. (8) can be written as a pair of equations for left and right channel audio signals, respectively, with superscripts L, R :

$$F_j^L(f) = \sqrt{\frac{\sum_{i=1}^N B_{ij}^L(f) \left(w_1(f) |H_{1,ij}^{REF}(f)|^2 G_{1,ij}^2(f) + w_2(f) |H_{2,ij}^{REF}(f)|^2 G_{2,ij}^2(f) + w_3(f) |H_{3,ij}^{REF}(f)|^2 G_{3,ij}^2(f) \right)}{\sum_{i=1}^N B_{ij}^L(f) \left(w_1(f) |H_{1,ij}^{REF}(f)|^2 + w_2(f) |H_{2,ij}^{REF}(f)|^2 + w_3(f) |H_{3,ij}^{REF}(f)|^2 \right)}}, \quad (9a)$$

$$F_j^R(f) = \sqrt{\frac{\sum_{i=1}^N B_{ij}^R(f) \left(w_1(f) |H_{1,ij}^{REF}(f)|^2 G_{1,ij}^2(f) + w_2(f) |H_{2,ij}^{REF}(f)|^2 G_{2,ij}^2(f) + w_3(f) |H_{3,ij}^{REF}(f)|^2 G_{3,ij}^2(f) \right)}{\sum_{i=1}^N B_{ij}^R(f) \left(w_1(f) |H_{1,ij}^{REF}(f)|^2 + w_2(f) |H_{2,ij}^{REF}(f)|^2 + w_3(f) |H_{3,ij}^{REF}(f)|^2 \right)}}. \quad (9b)$$

The modelling as described above using Eqs. (9) is applied to the finite-length screen case using a simplified set of binaural weights as depicted in Figure 5. The correspondingly produced sound has a clearly audible change in left–right balance as the train passes the end of the screen. No artefacts are noticed.

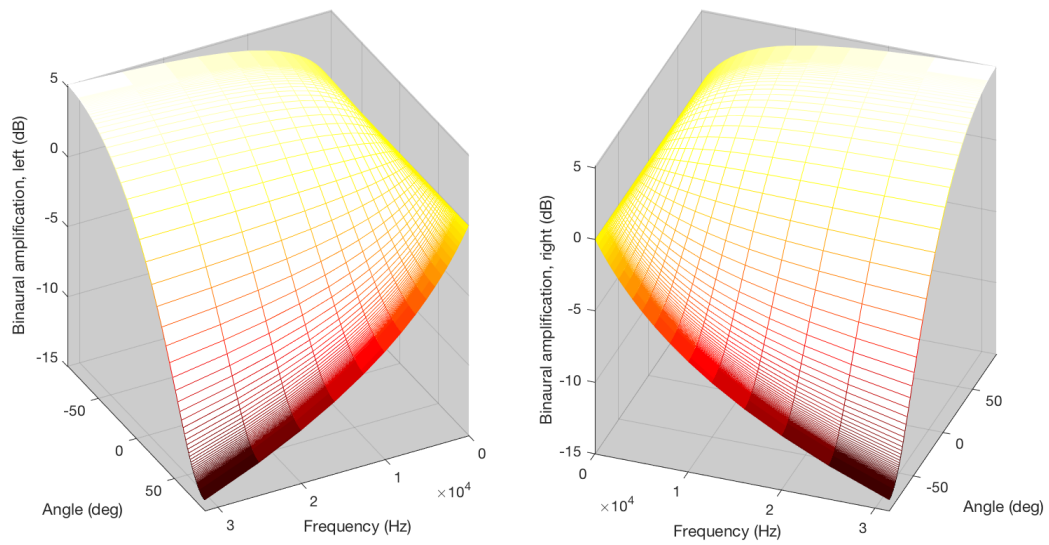


Figure 5. Example of simplified binaural weights, $B_{ij}(f)$, plotted as $10\log(B)$, as function of frequency and angle. (Left and right panels for left and right signals, respectively.)

REFERENCES

[1] Zhang X. Tuning of the acoustic source model: Aiming at accurate noise assessments along high-speed railways. 2015. (SP Rapport).

<http://urn.kb.se/resolve?urn=urn:nbn:se:ri:diva-5270>

[2] Zhang X. Prediction of high-speed train noise on Swedish tracks. 2010. (SP Rapport).

<http://urn.kb.se/resolve?urn=urn:nbn:se:ri:diva-4945>